COBEM 2021 26th International Congress of Mechanical Engineering
November 22-26, 2021, Virtual Congress, Brazil

COB-2021-1300
EXTRACTION OF STRESS INTENSITY FACTORS VIA THE DISPLACEMENT CORRELATION METHOD FROM STABLE GENERALIZED FINITE ELEMENT SOLUTIONS

Felipe Justino de Lima Lopes
Rafael Marques Lins
Mariano Andrés Arbelo
Instituto Tecnológico de Aeronáutica – São José dos Campos, Brazil
emails: felipe.bllopes@gmail.com, mlins@ita.com.br and marbelo@ita.br

Abstract. *This work presents and discuss the Stress Intensity Factors (SIF's) calculation using the Displacement Correlation Method (DCM) coupled to a Stable Generalized Finite Element Method (SGFEM). Moreover, the improvement of the results using the Stable Generalized Finite Element Method (SGFEM) instead of the Generalized Finite Element Method (GFEM) is also investigated. In these methods, in general, enrichment functions are applied to represent the effects of the singularity attached to the crack tip and the discontinuities introduced by the crack. Beyond that, the enrichment functions in the SGFEM are modified to avoid some problems that appear in the GFEM, as round off errors due to ill conditioning of the stiffness matrix, which can affect the convergence of the model. The DCM was chosen due to his low computational cost compared to other methods based on energetic approach such as the J integral. Such feature can be explored to implement fast crack growth simulations models using the SGFEM. Practical examples with closed form solution, considering different opening modes, are used to compare SIF's extracted using both SGFEM and GFEM methodologies. These examples include horizontal and inclined cracks aiming to demonstrate the robustness of the proposed technique.*

Keywords: *GFEM, SGFEM, Stress Intensity Factor, Displacement Correlation Method*

1. INTRODUCTION

This work aims to study the viability of the combination of the Displacement Correlation Method (DCM) and the Stable Generalized Finite Element Method (SGFEM) (Babuška and Banerjee, 2012) for computing accurate stress intensity factor (SIF) with low computational cost. Briefly, the SGFEM can be described as an improved variant of its predecessor, the Generalized Finite Element Method (Duarte *et al*., 2000). The reason to use this variant is justified because it exhibits all relevant features of its predecessor, like the capability to provide accurate solutions in the presence of cracks without the need of use a large number of elements or to reshape the mesh, adding a better control on the numerical conditioning. This last feature avoids round off errors that could come to affect the convergence rates (Babuška *et al*., 2013).

A reliable extraction of SIF's is extremely important in problems involving cyclic loads. Such problems are common in several structures, including aeronautical structures. The cracks nucleation due to fatigue cyclic loads, can lead to catastrophic failures (

Figure *1*) or unexpected maintenance tasks causing significant losses to the operators (Figure 2). Therefore, it is very important to have robust tools that are capable of ensure the safe and integrity of the structure for aeronautical applications.

(a) (b)

Figure 1. Effects arising from fatigue: (a) failure close the windows frames found on Havilland Comet crashes and (Diouf, 2013) (b) failure suffered by Aloha Airlines Boeing 737-200 (Airways Magazine, 2020).

Figure 2. Failures due to fatigue that cause unexpected maintenance tasks. (RPX Aviation, 2015)

2. METHODOLOGY

2.1 Stable Generalized Finite Elements Method

The Generalized Finite Elements Method consists in a numerical method based on Partition Unity concept (Melenk and Babuška, 1996). The main feature of this method is the augmentation of the classic approximation space from the FEM by means of a new space composed by the called enrichment functions. In the GFEM, the shape functions ($\Phi_{\alpha i}$) are defined inside a domain namely cloud (ω_α), composed by the elements which have one node in common called vertex. In this domain, the enrichment functions are multiplied by the lagrangian shape functions, i.e.:

$$\Phi_{\alpha i} = \varphi_\alpha L_{\alpha i} \tag{1}$$

where φ_α denotes the classic shape functions of the elements that belongs to cloud ω_α, $L_{\alpha i}$ denotes the i^{th} enrichment function coupled to cloud ω_α, with $i = 1, 2, \dots, nl$, where nl is the total number of enrichment functions.

Conventionally, the unity function is chosen as the first component of the set of enrichment functions. Then, considering a bidimensional model, the GFEM approximation applied to the displacement fields is given by:

$$\hat{u} = \sum_{\alpha=1}^{n} \varphi_\alpha u_\alpha + \sum_{\alpha=1}^{n} \varphi_\alpha \left(\sum_{\alpha=1}^{n} L_{\alpha i} b_{\alpha i} \right) \tag{2}$$

$$\hat{v} = \sum_{\alpha=1}^{n} \varphi_\alpha v_\alpha + \sum_{\alpha=1}^{n} \varphi_\alpha \left(\sum_{\alpha=1}^{n} L_{\alpha i} c_{\alpha i} \right) \tag{3}$$

On the equations above, n denotes the total number of clouds, u_α and v_α are the parameters associated to the degrees of freedom from classical finite elements and $b_{\alpha i}$ and $c_{\alpha i}$ are the parameters associated to the enrichment functions. An overview about the GFEM can be found in Fries and Belytschko (2010).

As previously mentioned, the application of GFEM may lead to some inconveniences, such as: the presence of blending elements (elements that are composed by enriched and not enriched nodes) and ill conditioning of the stiffness matrix. Aiming to overcome these problems, Babuška and Banerjee (2012) developed the Stable Generalized Finite Element Method. Basically, it consists of a modification in the original enrichment functions in such a way that it become zero on all nodes that composes the cloud associated to the enrichment. Hence:

$$L_{\alpha i}^{mod} = L_{\alpha i} - I_{\omega_\alpha}(L_{\alpha i}) \tag{4}$$

$$I_{\omega_\alpha}(x,y) = \sum_{j=1}^{ne} \varphi_j(x,y) L_{\alpha i}(x_j, y_j) \tag{5}$$

In Eq. (5), (x_j, y_j) denotes the coordinates of node *j* of the element and *ne* is the number of element nodes.

In analogous way to GFEM, the modified enrichment functions are multiplied by the lagrangian shape functions to generate the SGFEM shape functions, as can be seen in Eq. (6). Figure 3 depicts the application of the modified enrichment functions to generate the SGFEM shape functions.

$$\Phi_{\alpha i}^{mod} = \varphi_{\alpha i} L_{\alpha i}^{mod} \tag{6}$$

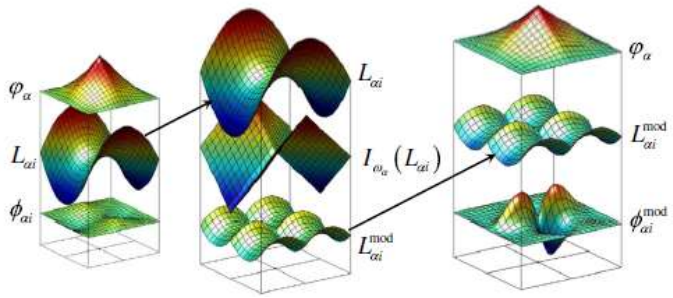

Figure 3. SGFEM shape functions representation (Adapted from Gupta *et al*. 2013)

2.2 Enrichment Functions

Moes *et al.* (1999) proposed to apply a degree type function to represent the displacement discontinuities in the region far from crack tip. These functions are represented by Eq. (7)

$$H(x,y) = \begin{cases} 1, y > 0 \\ -1, y \leq 0 \end{cases} \tag{7}$$

Gupta *et al* (2013) proposed the use of Linear Heaviside enrichment functions to ensure accurate results when using the SGFEM. These functions are indicated below:

$$H(x,y) = \left\{ H, H\frac{(x - x_\alpha)}{h_\alpha}, H\frac{(y - y_\alpha)}{h_\alpha} \right\} \tag{8}$$

where, x_α and y_α are the global cartesian coordinates of node *a* and h_α is a scaling factor given by the diameter of the largest element sharing the node.

Oden and Duarte (1997) proposed a set of trigonometric functions based on fracture mechanic solutions to enrich the nodes that are around the crack tip. These functions, known by "OD Branch Functions", are given by:

$$L_{OD-\bar{x}} = \left\{ \sqrt{r}\left[\left(\kappa - \frac{1}{2}\right) cos\frac{\theta}{2} - \frac{1}{2} cos\frac{3\theta}{2}\right], \sqrt{r}\left[\left(\kappa + \frac{3}{2}\right) sin\frac{\theta}{2} + \frac{1}{2} sin\frac{3\theta}{2}\right] \right\} \tag{9}$$

$$L_{OD-\bar{y}} = \left\{ \sqrt{r}\left[\left(\kappa + \frac{1}{2}\right) sin\frac{\theta}{2} - \frac{1}{2} sin\frac{3\theta}{2}\right], \sqrt{r}\left[\left(\kappa - \frac{3}{2}\right) cos\frac{\theta}{2} + \frac{1}{2} cos\frac{3\theta}{2}\right] \right\} \tag{10}$$

where, $\kappa = 3 - 4\nu$ for plane strain state and $\kappa = (3 - \nu)/(1 + \nu)$ for plane stress state, θ is the angle between the considered point relative to the crack tip and *r* is the distance of the considered point to the crack tip (see Figure 4).

The OD branch functions and the Linear Heaviside will be used as enrichment in the applications discussed in next section.

2.3 Stress Intensity Factor

The Stress Intensity Factor (SIF) depends on some features like crack length, displacement field around crack tip and crack growth mode. Although the regions near to the crack tip can have a plastic behavior, only the elastic effects will be considered hereby. Thus, the SIF's will be calculated using the Linear Elastic Fracture Mechanics concepts. Following will be presented two ways to compute the SIF's.

(a) Displacement Correlation Method (DCM)

According to Westgaard (1939) it is possible to describe the displacement field around the crack tip as:

$$u = \frac{K_I}{2\mu}\sqrt{\frac{r}{2\pi}}cos\left(\frac{\theta}{2}\right)\left[(\kappa-1)+2sin^2\left(\frac{\theta}{2}\right)\right]+\frac{K_{II}}{2\mu}\sqrt{\frac{r}{2\pi}}sin\left(\frac{\theta}{2}\right)\left[(\kappa+1)+2cos^2\left(\frac{\theta}{2}\right)\right] \tag{11}$$

$$v = \frac{K_I}{2\mu}\sqrt{\frac{r}{2\pi}}sin\left(\frac{\theta}{2}\right)\left[(\kappa+1)+2cos^2\left(\frac{\theta}{2}\right)\right]+\frac{K_{II}}{2\mu}\sqrt{\frac{r}{2\pi}}cos\left(\frac{\theta}{2}\right)\left[(\kappa-1)+2sin^2\left(\frac{\theta}{2}\right)\right] \tag{12}$$

where μ is the shear modulus. The SIF can be computed by the difference between the displacements on the crack faces. Thus, replacing $\theta = \pi$ and $\theta = -\pi$ in the Eq. (11) and Eq. (12), respectively:

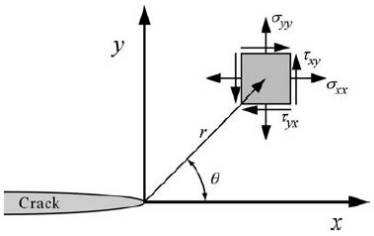

Figure 4. Stress fields definition around the crack tip (Anderson, 2005).

$$K_I = \sqrt{\frac{2\pi}{r}}\frac{\mu}{(\kappa+1)}COD \tag{13}$$

$$K_{II} = \sqrt{\frac{2\pi}{r}}\frac{\mu}{(\kappa+1)}CSD \tag{14}$$

In Eq. (13), COD (Crack Opening Displacement) is the difference between the displacements perpendicular to crack face, whereas that in Eq. (14), CSD (Crack Sliding Displacement) corresponds to the difference between the displacements parallel to the crack faces.

Gupta *et al.* (2017) proposed the application of a linear least square extrapolation to improve the accuracy of the DCM. This method can be summarized by means of the following equation:

$$\boldsymbol{Ac} = \overline{\boldsymbol{y}} \tag{15}$$

where:

$$\boldsymbol{A} = \boldsymbol{X^T X} \tag{16}$$

$$\overline{\boldsymbol{y}} = \boldsymbol{X^T y}$$

$$\boldsymbol{c} = \begin{bmatrix} c_0 \\ c_1 \end{bmatrix} \tag{17}$$

$$\boldsymbol{y} = \begin{bmatrix} K_{I,r_1} \\ \vdots \\ K_{I,r_{N_{LS}}} \end{bmatrix} \tag{18}$$

$$\boldsymbol{X} = \begin{bmatrix} 1 & r_1 \\ \vdots & \vdots \\ 1 & r_{N_{LS}} \end{bmatrix} \tag{19}$$

Thus, the extrapolated value for K_I is obtained at *r=0*, i.e.:

$$K_I = K_I^{LS}(0) = c_0 \tag{20}$$

The number of radii adopted hereby in the extrapolation procedure (N_{LS}) was defined as *30%* of the crack length. An analogous procedure can be used for computing the extrapolated value for K_{II}.

(b) J Contour Integral Method

Rice (1968) defined the J Contour Integral by:

$$J = \int_{\Gamma} \left(w dy - T_i \frac{\partial u_i}{\partial x} ds \right) \tag{21}$$

where:

- w = Strain Energy Density (see Eq. (22));
- T_i = Components of the traction vector (see Eq. (23));
- u_i = Components of the displacement vector;
- ds = Incremental length in contour Γ (see
- *Figure 5*).

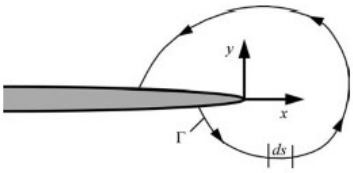

Figure 5. Arbitrary contour around the crack tip (Anderson, 2005).

$$w = \int_0^{\varepsilon_{ij}} \sigma_{ij} d\varepsilon_{ij} \tag{22}$$

$$T_i = \sigma_{ij} n_j \tag{23}$$

Therefore, for a linear elastic material, the SIF can be calculated according to Eq (24) and Eq. (25) for mode I and mixed mode respectively.

$$J = \frac{K_I^2}{E'} \tag{24}$$

$$J = \frac{K_I^2}{E'} + \frac{K_{II}^2}{E'} \tag{25}$$

where, $E^{'} = E$ for plane stress state and $E' = \frac{E}{1-\nu^2}$ for plane strain state (E is the Young modulus).

At least, an arithmetic average is applied to the SIF's obtained by J Contour Integral using thirty circular paths with radius varying between *20%* and *50%* relative to crack length. More details about this procedure for computing SIF's via J integral can be found in Cotta (2016).

3. NUMERICAL RESULTS

With the objective to validate the implementation of the DCM and J Integral Contour Method, as well as to compare the GFEM and the SGFEM, will be analyzed three benchmark problems: tensile edge crack, shear edge crack and inclined centered crack (see

Figure *6*). For the two first problems, four meshes are adopted aiming to investigate the convergence of the results. These meshes present the following grid sizes: 5x10, 10x20, 20x40, 40x80 in the tensile edge crack case. On the other hand, in the shear edge crack, the grid sizes are: 12x24, 19x39, 39x79, 79x159. In the last case, only one mesh is investigated with a grid size equal to 20x40.

All the numerical results evaluated in this section were computed using the GFEM/SGFEM dedicated objected-oriented programming toolkit named SCIEnCE, described in the work of Borges (2017).

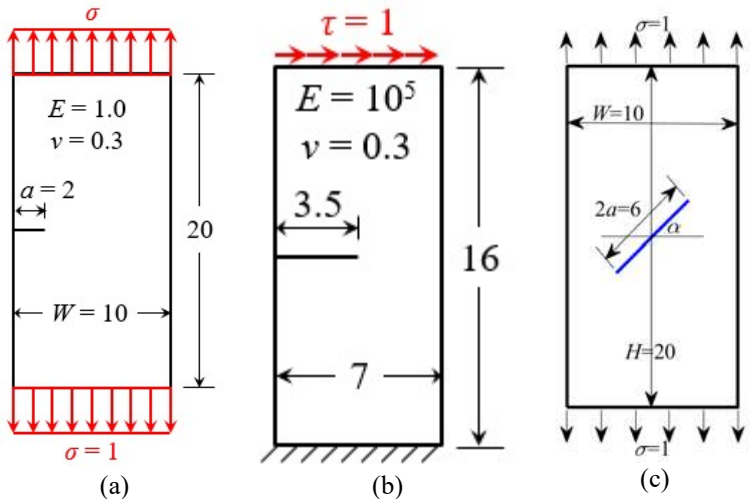

Figure 6. Benchmark problems. (a): tensile edge crack; (b): shear edge crack; (c): inclined centered crack.

Figure 7 shows the one of adopted meshes with its respective enriched nodes for the problem with tensile edge crack. It was applied Linear Heaviside enrichment functions on the nodes surrounding the crack and far from the crack tip and OD Branch Functions on the nodes located in a circular region with radius equal to 1 around the crack tip.

Figure *8* shows the adopted mesh with its respective enriched nodes for the problem with inclined centered crack. It was applied Linear Heaviside enrichment functions on the nodes surrounding the crack and far from the crack tip and OD Branch Functions on the nodes located in a circular region around the crack tip with radius equal to *30%* of crack length.

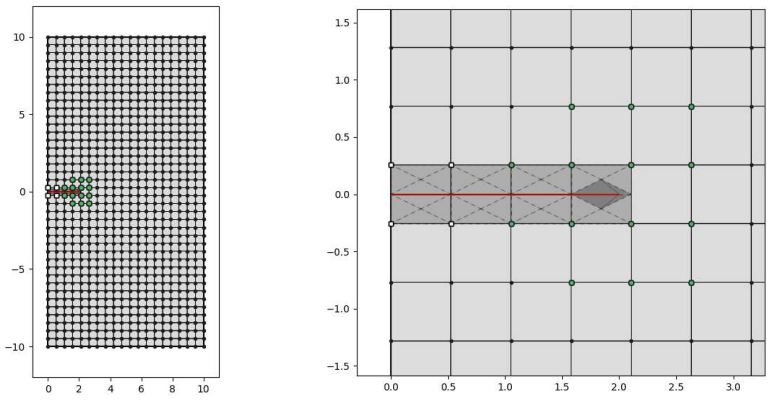

Figure 7. Tensile corner cracked panel. Green nodes enriched with OD branch functions and white nodes enriched with Linear Heaviside Functions.

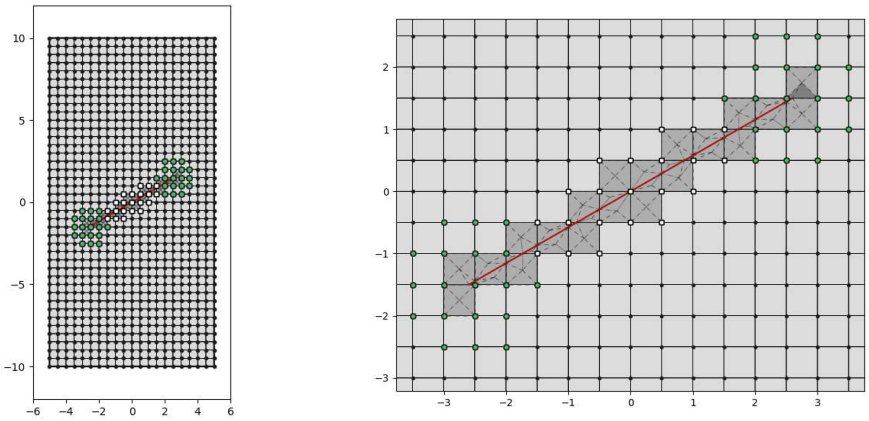

Figure 8. Centered inclined cracked panel. Green nodes enriched with Branch Functions and red nodes enriched with Heaviside Functions.

Figure 9 to Figure 11 show the relative error between the calculated SIF and the one extracted from the open literature for the two first analyzed benchmark problems. The reference values came from Ewalds and Wanhill (1989).

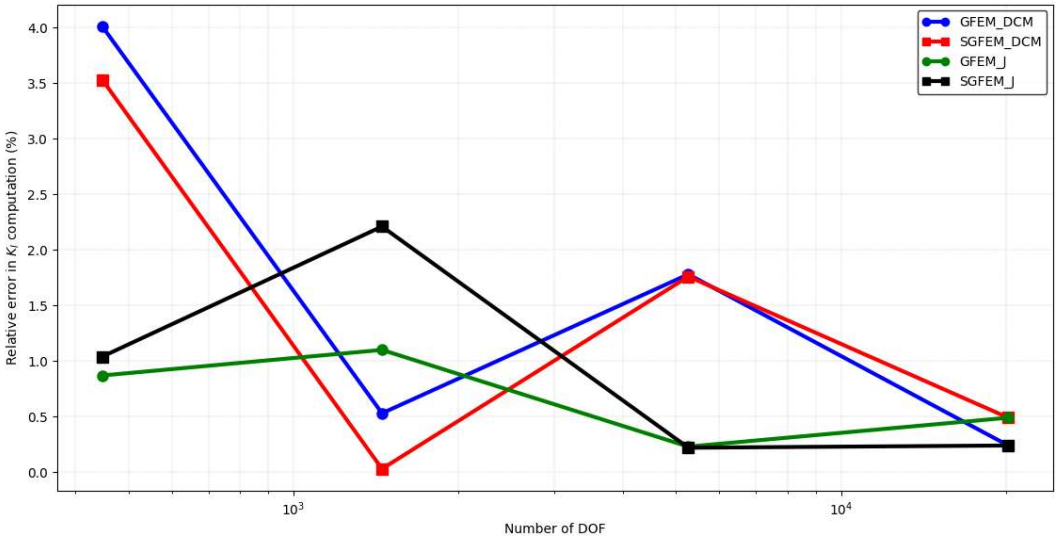

Figure 9. SIF comparison between GFEM and SGFEM for tensile edge crack.

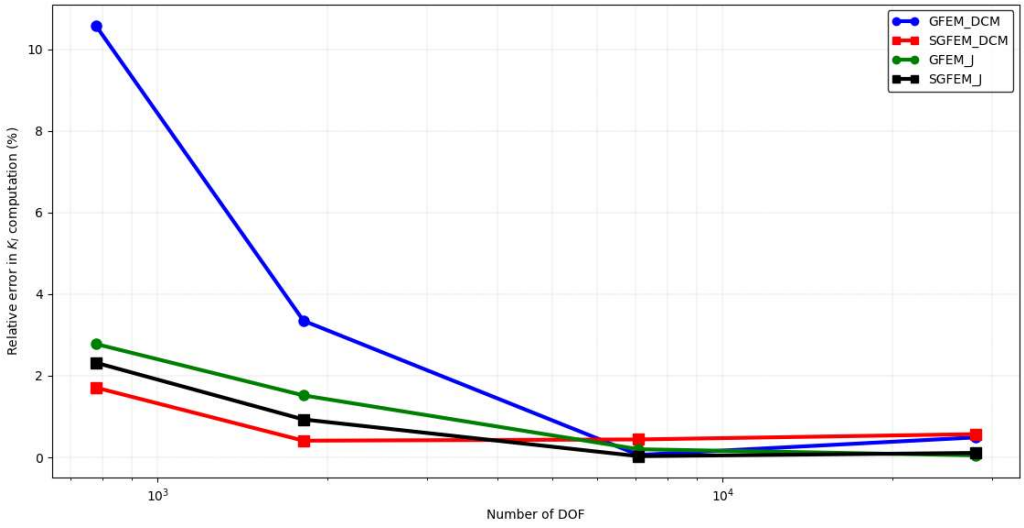

Figure 10. SIF comparison between GFEM and SGFEM - Mode I - Shear edge crack.

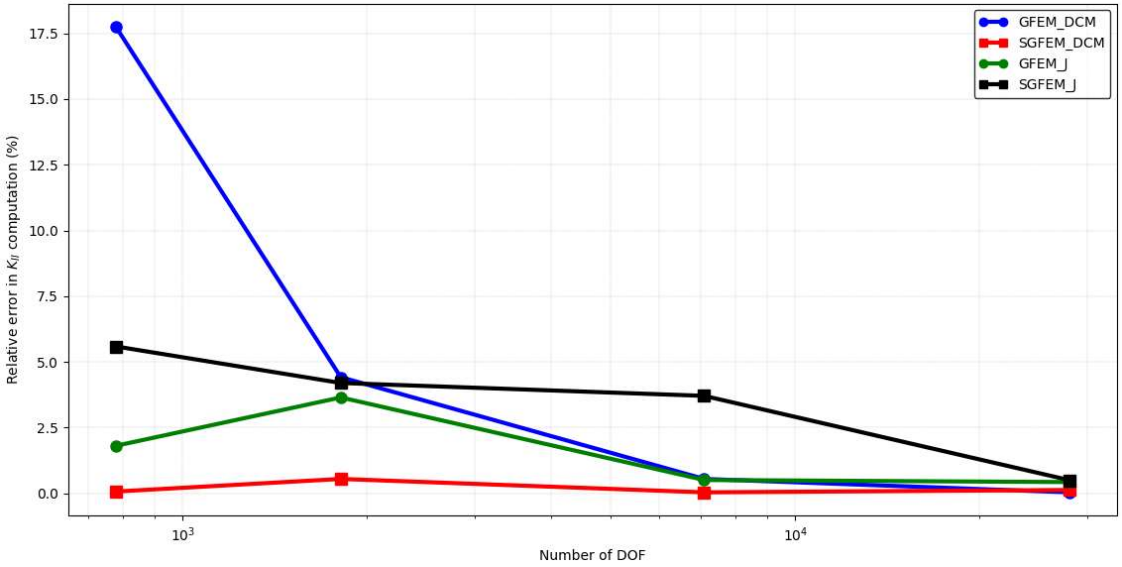

Figure 11. SIF comparison between GFEM and SGFEM - Mode II - Shear edge crack.

Table 1 and
Table *2* present the relative errors for the analyses performed.

Table 1. Relative error of Stress Intensity Factor for tensile edge crack.

Number of DOF	GFEM		SGFEM	
	KI_DCM	KI_J	KI_DCM	KI_J
448	4.01%	0.87%	3.53%	1.04%
1452	0.53%	1.10%	0.03%	2.21%
5264	1.78%	0.23%	1.76%	0.22%
20204	0.24%	0.49%	0.49%	0.24%

Table 2. Relative error of Stress Intensity Factor for shear edge crack.

Number of DOF	GFEM		SGFEM		GFEM		SGFEM	
	KI_DCM	KI_J	KI_DCM	KI_J	KII_DCM	KII_J	KII_DCM	KII_J
778	10.51%	2.78%	1.71%	2.32%	17.74%	1.81%	0.07%	5.59%
1812	3.35%	1.52%	0.41%	0.93%	4.42%	3.65%	0.55%	4.20%
7100	0.06%	0.20%	0.44%	0.03%	0.55%	0.51%	0.04%	3.71%
28056	0.49%	0.05%	0.57%	0.11%	0.04%	0.43%	0.13%	0.50%

The results above have demonstrated that the DCM, when combined with the linear least square extrapolation technique, can extract SIF values with very low relative error. Furthermore, when analyzing the results from second benchmark problem, it can be verified that SGFEM has improved the SIF when using DCM technique.

Figure 12 and
Figure *13* show the relative error between the calculated SIF and the one extracted from the open literature for the analyses performed for inclined centered crack using only the DCM applying the linear least square extrapolation technique described above. The reference values were extracted from Marukami (1987).

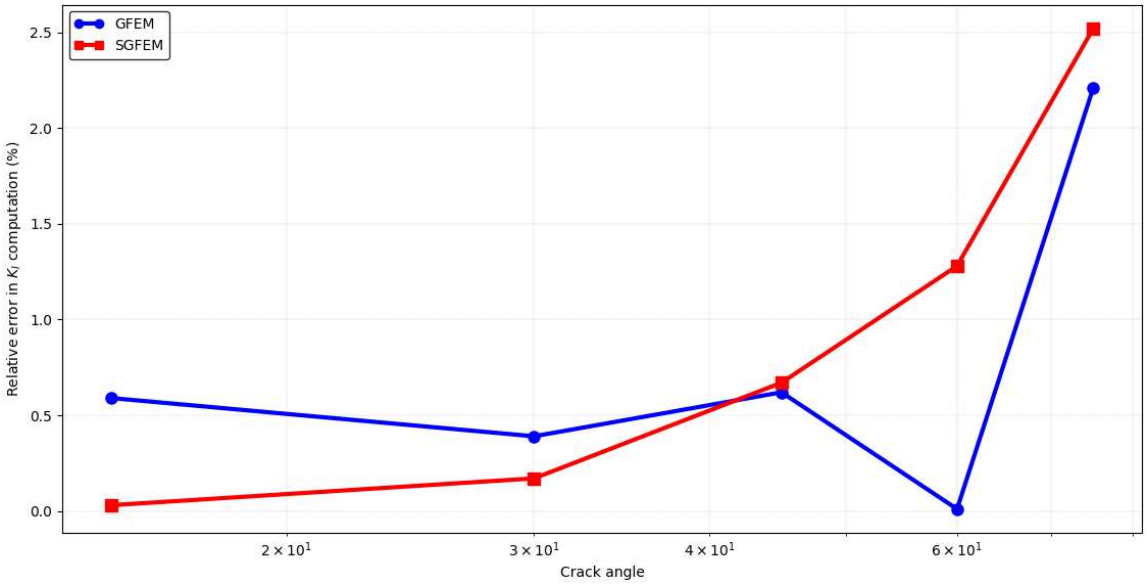

Figure 12. SIF comparison between GFEM and SGFEM - Mode I - Inclined centered crack.

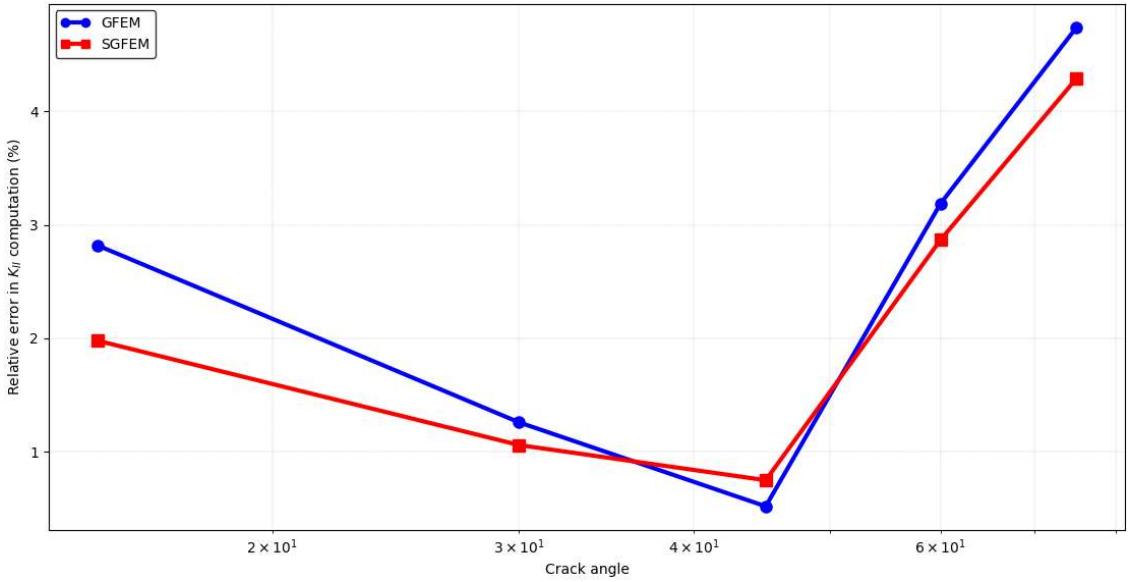

Figure 13: SIF comparison between GFEM and SGFEM - Mode II - Inclined centered crack.

Table 3 shows that the application of linear least square extrapolation technique has improved the results as we can observe the low values of SIF's relative errors for inclined centered crack plate. Moreover, it can be observed that the relative errors increase with the raise of the crack angle. The reason for this is that the shear effects are more significant in the cases with the crack angles greater than 45° and, according to Anderson (2005), the Westgaard equations has some restrictions when applied for calculation of mode II predominant.

Table 3. Error relative for inclined centered crack considering DCM.

Crack Angle	GFEM		SGFEM	
	K_I	K_{II}	K_I	K_{II}
15°	0.59%	1.98%	0.03%	2.82%
30°	0.39%	1.06%	0.17%	1.26%
45°	0.62%	0.75%	0.67%	0.52%
60°	0.01%	2.87%	1.28%	3.19%
75°	2.21%	4.29%	2.52%	4.74%

4. CONCLUSIONS

The results obtained from the work presented and discussed on this paper allow us to conclude that the SGFEM generated consistent results, when compared with the results obtained from close form solutions available on the open literature. Furthermore, in most cases, when the DCM is applied combined with least linear square extrapolation technique, the SGFEM provided more accurate results than its predecessor, the GFEM.

Furthermore, it is demonstrated that, despite of the simplicity involved at its formulation, when compared to the other extraction techniques, the application of the DCM provided results that are close to the references when combined with the linear least square extrapolation technique.

5. ACKNOWLEDGMENTS

This work was supported by CNPq Grant No. 311972/2020-9.

6. REFERENCES

Addressing the Root Cause of Aircraft Structure. RPX Aviation, 2015 *(web publications)*, https://www.rpxtech.com/blog/addressing-the-root-cause-of-fatigue.

Aloha Airlines Flight 243 Incident, 32 Years Later. Airways Magazine, 2020 *(web publications)*, https://airwaysmag.com/airlines/32-years-aloha-flight-243-accident.

Anderson, T. L., 2005 Fracture Mechanics – Fundamentals and Applications (3ed), CRC Press.

Babuška, I., Banerjee, U., 2012 "Stable Generalized Finite Element Method (SGFEM)". *Comput. Methods Appl.Mech. Engineering*. 201-204, pp. 91-111.

Babuška, I., Banerjee, U., Gupta, V., Duarte, C.A., 2013 "A Stable and Optimally Convergent Generalized FEM (SGFEM) for Linear Elastic Fracture Mechanics" *Comput. Methods Appl.Mech*. 266, pp. 23-39.

Borges, L., P., 2017 *Método dos Elementos Finitos Generalizados na análise de integridade estrutural de interesse para indústria aeronáutica* (in Portuguese). Master's Thesis, São Carlos School of Engineering, São Carlos, Brazil

Cotta, I., 2016 *Splitting Method in Multisite Damage Solids: Mixed Mode Fracturing and Fatigue Problems.* PHD Thesis, São Carlos School of Engineering, São Carlos, Brazil.

Duarte, C., A., Babuška, I., Oden, J., T., 2000 "Generalized Finite Element Methods for Three-Dimensional Structural Mechanics Problems" *Comput Struct*.77, pp. 215-232.

Diouf, B., 2013 *(web publications)* Stress Concentration! EMCH407 – Numerical Analysis, https://tecnoblog.net/247956/referencia-site-abnt-artigos.

Ewalds, H., Wanhill, R., 1989 "Fracture Mechanics"; Edward Arnold: New York.

Fries, T.P., Belytschko, T., 2010 "The generalized/extended finite element method: An overview of the method and its applications" *International Journal for Numerical Methods in Engineering,* Vol. 82, pp. 1044-1072.

Gupta, V., Duarte, C. A., Babuška, I., Banerjee, U., 2013 "A stable and optimally convergent generalized FEM (SGFEM) for linear elastic fracture mechanics" *Computer Methods in Applied Mechanics and Engineering,* Vol 266, pp. 23-39.

Gupta, P., Duarte, C.A., Dhankhar, A., 2017 "Accuracy and Robustness of Stress Intensity Factor Extraction Methods for the Generalized/eXtended Finite Element Method" *Engineering Fracture Mechanics,* pp.120-153.

Gupta, P., Pereira, J.P., Kim D-J, Duarte, C.A., Eason, T., 2012 "Analysis of three-dimensional fracture mechanics problems: A non-intrusive approach using a generalized finite element method". *Engng Fract Mech,* 90: pp. 41-64.

Marukami Y., 1987 Stress Intensity Factors Handbook, Pergamon Press, Oxford.

Melenk, J., M., Babuška, I., 1996 "The Partition of Unity Finite Element Method: Basic Theory and Applications". *Comput Methods Appl Mech Eng*. 139, pp. 289-314.

Moes, N., Dolbow, J., Belytschko, T., 1999 "A finite element method for crack growth without remeshing" *International Journal for Numerical Methods in Engineering*, Vol. 46, No. 1, pp. 131-150.

Oden, J. T., Duarte, C. A., 1997 "Chapter: clouds, cracks and FEM's. In *Recent Developments in Computational and Applied Mechanics,* pp. 302-321.

Rice, J.M., 1968 "A Path Independent Integral and the Approximate Analysis of Strain Concentration by Notches and Cracks". *Journal of Applied Mechanics,* Vol. 35, pp. 379-386.

Westgaard, H.M., 1939 "Bearing Pressures and Cracks." *Journal of Applied Mechanics,* Vol. 6, pp. 49-53.

7. RESPONSIBILITY NOTICE

The authors are the only responsible for the printed material included in this paper.